INTERNATIONAL JOURNAL OF HYDROGEN ENERGY 43 (2018) 9046–9058

Available online at www.sciencedirect.com

ScienceDirect

journal homepage: www.elsevier.com/locate/he

Hydrogen-diesel fuel co-combustion strategies in light duty and heavy duty CI engines

Midhat Talibi [a,*], *Paul Hellier* [a], *Robert Morgan* [b], *Chris Lenartowicz* [b], *Nicos Ladommatos* [a]

[a] *Department of Mechanical Engineering, University College London, Torrington Place, London WC1E 7JE, United Kingdom*

[b] *School of Computing, Engineering and Mathematics, University of Brighton, Cockcroft Building, Lewes Road, Brighton, BN2 4GJ, United Kingdom*

ARTICLE INFO

Article history:
Received 30 November 2017
Received in revised form
19 February 2018
Accepted 24 March 2018
Available online 13 April 2018

Keywords:
Hydrogen
Co-combustion strategies
Diesel engine
Light duty
Heavy duty
EGR
Exhaust emissions

ABSTRACT

The co-combustion of diesel fuel with H_2 presents a promising route to reduce the adverse effects of diesel engine exhaust pollutants on the environment and human health. This paper presents the results of H_2-diesel co-combustion experiments carried out on two different research facilities, a light duty and a heavy duty diesel engine. For both engines, H_2 was supplied to the engine intake manifold and aspirated with the intake air. H_2 concentrations of up to 20% vol/vol and 8% vol/vol were tested in the light duty and heavy duty engines respectively. Exhaust gas circulation (EGR) was also utilised for some of the tests to control exhaust NO_x emissions.

The results showed NO_x emissions increase with increasing H_2 in the case of the light duty engine, however, in contrast, for the heavy duty engine NO_x emissions were stable/reduced slightly with H_2, attributable to lower in-cylinder gas temperatures during diffusion-controlled combustion. CO and particulate emissions were observed to reduce as the intake H_2 was increased. For the light duty, H_2 was observed to auto-ignite intermittently before diesel fuel injection had started, when the intake H_2 concentration was 20% vol/vol. A similar effect was observed in the heavy duty engine at just over 8% H_2 concentration.

Introduction

Policy makers and the general public alike are increasingly aware of, and concerned by, the negative impacts of IC engine exhaust gas species on urban air quality and human health [1]. Recent attention has focused on levels of both nitrogen oxides (NOx) and particulate matter (PM) emitted by diesel engine powered vehicles, with higher mortality rates being attributed to PM emissions alone in urban cities. Cities across the world are now moving to establish ultra-low emission zones, and four major cities worldwide have announced plans to ban diesel powered vehicles from 2025 [2]. Future fuel and combustion strategies for IC engines must therefore be designed such that the necessary reductions in pollutant emissions can be met, while also addressing the need to reduce net greenhouse gas emissions [3–5].

* *Corresponding author.*
E-mail addresses: m.talibi@ucl.ac.uk, midhattalibi@hotmail.com (M. Talibi).
https://doi.org/10.1016/j.ijhydene.2018.03.176

Mitigating the adverse impacts of exhaust pollutants from light and heavy duty diesel engines alike is challenging; both in the context of the range of diesel powered vehicle applications and the inherent complications that arise from after-treatment of compression ignition exhaust relative to that from spark ignition combustion. Large vans, trucks and lorries are required to operate both in urban and extra-urban environments and utilise diesel engines of various sizes, the replacement of which with electric and hybrid power units is less imminent than in the case of SI engine powered passenger vehicles [6–9]. Meanwhile, the often locally rich but globally lean stoichiometry of diesel combustion [10] results in elevated levels of PM and excess oxygen in engine exhaust gases that necessitate the use of several after-treatment systems in series for effective reduction of pollutant emissions. One possibility for the reduction of PM formation during combustion [11], and to lower the burden on after-treatment devices, is the use of alternative fuels other than fossil diesel. The use of biofuels is a potential opportunity for the reduction of PM emissions by this approach (in addition to the possibility of reducing GHG emissions from the transport sector) as they often contain oxygen, the presence of which within a fuel molecule can reduce the availability of fuel carbon for soot formation [12], and do not typically contain high sooting tendency aromatic molecules [13]. Fatty acid esters derived from vegetable oils (and commonly referred to as biodiesel) have been widely considered for the displacement of fossil diesel fuel [14]. While the use of biodiesels, either in blends with fossil diesel or unblended, has often resulted in reduced particulate emissions relative to straight fossil diesel, in many studies concurrent increased NOx emissions have also been observed [15,16]. However, studies utilising potential biofuels containing a higher proportion of oxygen than long chain fatty acid esters, for example ethers and short chain alcohols, in blends with fossil diesel and biodiesel have reported simultaneous reductions in both PM and NOx [17,18]. In addition to oxygen bearing fuels, a further approach that has been considered for the reduction of PM in particular has been the partial displacement of fossil diesel or biodiesel with fuels of lower carbon content, for example with co-combustion of natural gas [19] or hydrogen [20–22].

Several H_2-diesel fuel co-combustion studies have been conducted in literature with the hydrogen introduced in the intake manifold, and thus aspirated into the combustion chamber with the intake air [23–27]. Co-combustion studies undertaken on naturally aspirated engines have reported reductions in exhaust emissions of NOx and particulates at low H_2 substitution levels, however, at higher H_2 substitution levels, an increase in both exhaust NOx and particulate emissions has been observed [26–28]. NOx emissions were speculated to increase due to higher in-cylinder gas temperatures resulting from H_2 combustion, while particulate emissions increased due to displacement of intake O_2 by H_2. Some researchers have attempted to mitigate these effects by utilising exhaust gas recirculation (EGR) and intake air boost with H_2-diesel co-combustion [29–32]. Miyamoto et al. [29] studied the effect of EGR with H_2-diesel co-combustion, and was able to achieve simultaneous reductions in smoke and NO_x emissions. Roy et al. [31] managed to achieve a 90% energy substitution of diesel by H_2 in a supercharged engine, with N_2 utilised as simulated EGR to dilute the intake air. The authors were able to operate the engine at 42% brake thermal efficiency, with negligible levels of NO_x and smoke emitted. More recently, Wu et al. [33] investigated the effect of elevated intake air temperature on an engine operating on H_2 and diesel fuel. Although a considerable reduction in exhaust emissions was achieved (41% NO_x and 30% smoke emissions reduction), no significant impact of intake air temperature on engine performance and emissions was observed by the authors.

More recently, Pana et al. [34] investigated the effect of H_2 fuelling on the efficiency and emissions parameters of a truck diesel engine. The authors reported a 10% reduction in break specific energy consumption (BSEC), a 5.5% reduction in NO_x emissions and considerable reduction smoke and soot emissions, with the engine operating on 3.9% energy substitution by H_2 relative to diesel only engine operation. This in contrast to the work of Liu et al. [35] who, in aspirating H_2 to the intake of a heavy duty diesel engine, observed a reduction in brake thermal efficiency (BTE) and increase in NO_2 emissions arising from poor H_2 combustion efficiency and significant H_2 slip to the exhaust, with the presence of unburnt H_2 suggested to have enhanced the conversion of NO to NO_2. Liew et al. [36] also observed low H_2 combustion efficiency when aspirated into the intake of a heavy duty diesel engine, and at high loads for the addition of H_2 to result in significant increases in peak heat release rates during diffusion controlled combustion. Morgan et al. [37] observed a relatively minor reduction in BTE (~1%) when undertaking H_2-diesel co-combustion in a heavy duty engine, attributed to higher diesel fuel direct injection pressures (of up 3000 bar) that enhanced mixing of diesel fuel with the air-H_2 mixture and resulted in higher levels of H_2 combustion efficiency.

However, H_2 combustion in diesel engines can lead to issues such as uncontrolled ignition, surface ignition and backfiring, and high rates of heat release leading to knock. Tsujimura and Suzuki (2017) recently conducted a detailed study on the phenomenon of abnormal combustion (auto-ignition of H_2) in a hydrogen-fuelled diesel engine. At low engine loads, the authors did not observe any apparent evidence of H_2 combustion in the heat release rate. However, at higher loads and higher H_2 fractions, the start of combustion was observed to advance. Abnormal combustion of H_2 was observed when the H_2 fraction was above 50% under high load engine operation. At these conditions, the cylinder head temperature was also observed by the authors to be strongly dependent on H_2 fraction, probably due to increased flame propagation speeds of H_2 with increasing H_2 fraction.

Hydrogen has also been utilised as a fuel for homogenous charge compression ignition combustion (HCCI), where controlled autoignition of the intake aspirated H_2 close to engine TDC is required [38–40]. This was achieved, for example, by Ibrahim and Ramesh [41] in a single cylinder CI engine where H_2 was aspirated into preheated air at 120 °C to 130 °C. As the fraction of H_2 aspirated into the intake, and thus the equivalence ratio, was increased an advance in the start of combustion (SOC) and higher peak heat release rates were observed, until an engine load of 2.2 bar BMEP (brake mean effective pressure), after which knocking (uncontrolled H_2 ignition) occurred.

The above review of literature shows that while a variety of work has been conducted in H_2-diesel co-combustion, there is

Table 1 – Light duty diesel engine specifications.

Bore	86 mm
Stroke	86 mm
Swept volume	499.56 cm^3
Compression ratio (geometric)	18.3: 1
Maximum in-cylinder pressure	150 bar
Piston design	Central ω – bowl in piston
Fuel injection pump	Delphi single-cam radial-piston pump
High pressure common rail	Delphi solenoid controlled, 1600 bar max.
Diesel fuel injector	Delphi DFI 1.3 6-hole solenoid valve
Electronic fuel injection system	1 μs duration control
Crank shaft encoder	1800 ppr, 0.2 CAD resolution
Oil and coolant temperature	80 ± 2.5 °C

Table 2 – Heavy duty diesel engine specifications.

Bore	131.1 mm
Stroke	150 mm
Compression ratio	16:1
Swept volume	2 l
Swirl	Quiescent
Combustion chamber	Open Chamber
Diesel injection system	Delphi F2E Pumped Injector

still a need for a comprehensive study which looks into the addition of H_2 from very low levels up to the levels at which H_2 starts autoigniting. It is also important to understand if H_2 combustion has similar effects in light and heavy duty diesel engines, or do the different engine geometry, engine load, injection pressures, etc. have a significant effect, and therefore different H_2 combustion strategies are required. This paper presents results of H_2 diesel fuel co-combustion experiments in both a light duty and heavy duty engine diesel. Intake aspirated H_2 concentrations of up 20% vol/vol and 8% vol/vol were tested in the light duty and heavy duty engines respectively so as to study the effects of H_2 on combustion phasing, including autoignition, and exhaust emissions.

Experimental setup

The hydrogen-diesel fuel co-combustion tests were carried out at two different experimental facilities, a light duty diesel engine at UCL and a heavy duty diesel engine at University of Brighton. The details of both setups have been described in the following sections.

Light duty diesel engine

The light duty tests were carried out on a 4-stroke, single cylinder, direct injection compression-ignition engine consisting of a 4 cylinder, 2.0 L Ford Duratorq head, valves, piston and connecting rod from a donor engine, mounted on a single cylinder Ricardo Hydra crankcase. The facility has been described in detail in previous publications [27,30], and Table 1 lists some of the specifications of the setup. The head was fitted with a piezoelectric pressure transducer (Kistler 6056A) coupled to a charge amplifier (Kistler 5018), to measure the in-cylinder gas pressures to a resolution of 0.2 CAD. The in-cylinder pressure was pegged to the intake manifold pressure at the piston intake BDC position every engine cycle. One dimensional thermodynamic models were utilised to derive heat release rates from the measured in-cylinder pressures. Various other pressures (intake manifold, exhaust, etc.) and temperatures (oil, coolant, intake, exhaust, etc.), were also measured and logged onto PCs using National Instruments data acquisition systems (NI DAQ). Diesel fuel was injected into the cylinder using a six-hole, servo-hydraulic fuel injector, with the injection parameters (injection pressure (±1 bar), injection timing (±0.1 CAD) and duration of injection (±1 μs) controlled with an open loop ECU (Emtronix EC-

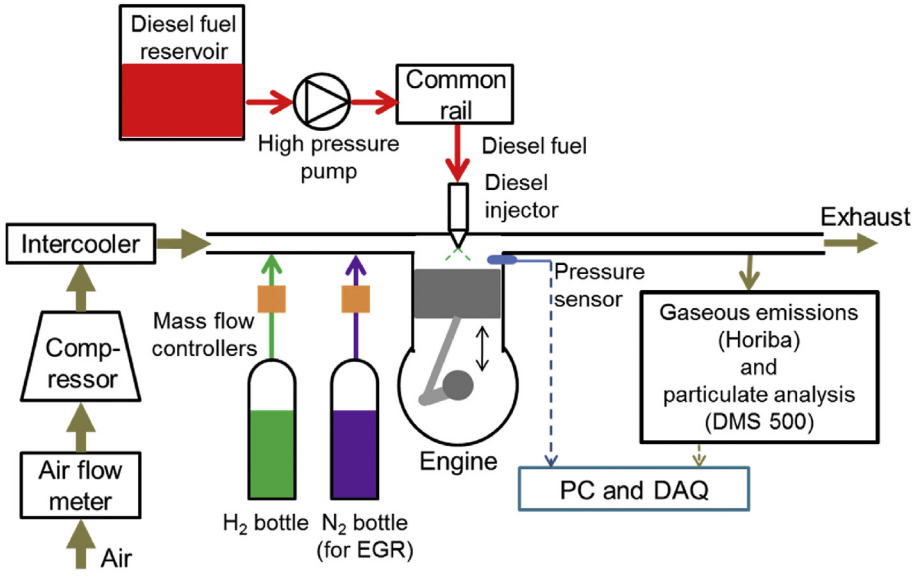

Fig. 1 – Schematic of the light duty diesel engine test facility including the supercharger setup and exhaust analysis systems.

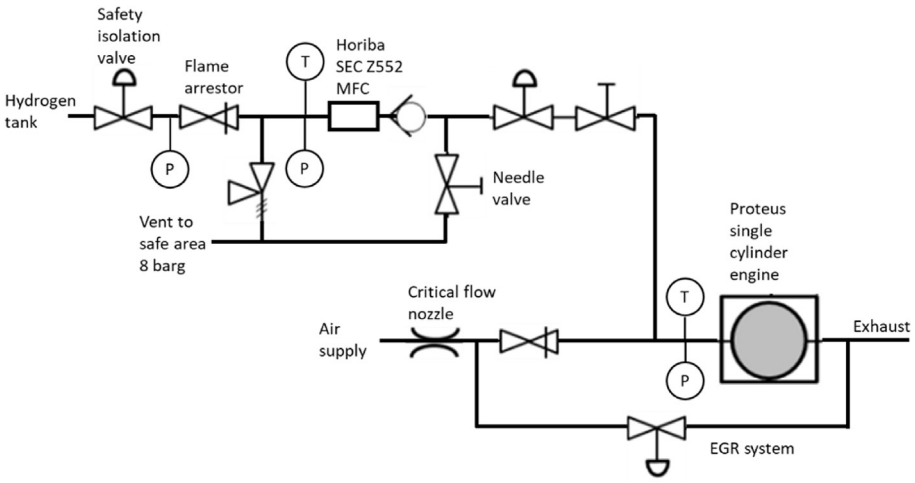

Fig. 2 – Schematic of heavy duty diesel engine setup.

Table 3 – Densities and lower heating values of diesel fuel and hydrogen at 1 atm and 300 K [8].

Property	Diesel fuel	Hydrogen
Density (kg/m^3)	831.9	0.0838
Lower heating value (MJ/kg)	43.14	120

GEN500). H_2 was supplied from a compressed gas cylinder supplied by BOC, and fed into the engine intake manifold 350 mm upstream of the intake valves, from where it was aspirated with the intake air into the engine. The flow of H_2 was controlled with a Bronkhorst thermal mass flow meter (F-201AV-70K), to an accuracy of ±0.08 l/min over the engine range. N_2 gas was supplied from another compressed gas cylinder to the engine intake manifold to simulate EGR-like conditions inside the cylinder by reducing the concentration of intake O_2. The flow of N_2 was controlled using a separate mass flow controller F-202AV-70K, to an accuracy of ±0.15 l/min over the entire range.

Exhaust gas emissions were collected 300 mm downstream of the exhaust valves and transferred, via a heated line maintained at 190 °C, to a Horiba automotive exhaust gas analyser rack (MEXA-9100HEGR) for the measurement of CO and CO_2 (non-dispersive infrared absorption analyser), NO_x (chemiluminescence analyser), unburned THC (flame ionization detector) and O_2 concentrations (magneto-pneumatic analyser). In addition, the number and size distribution of exhaust gas particulates was measured using a Cambustion particulate spectrometer (DMS500). Fig. 1 shows the schematic of the experimental setup for the light duty diesel engine.

Heavy duty diesel engine

The heavy duty diesel engine tests were conducted on a Ricardo Proteus, described in Ref. [37] and key parameters summarised in Table 2. The combustion chamber was of the quiescent open chamber type, typical of modern heavy duty diesel engines. A Delphi FRE pumped injection system was used for fuel delivery, which was capable of 3000 bar fuel injection pressures. The test facility was modified to convert the engine for hydrogen fumigation of the intake system (Fig. 2). This included a flame arrestor and bursting disk in the intake system of the hydrogen injection system. A Horiba SEC Z552MGX mass flow controller was used to regulate the flow of hydrogen into the intake system of the engine. The hydrogen was introduced well upstream of the intake ports in a bend via a perforated tube to promote good mixing with the charge air.

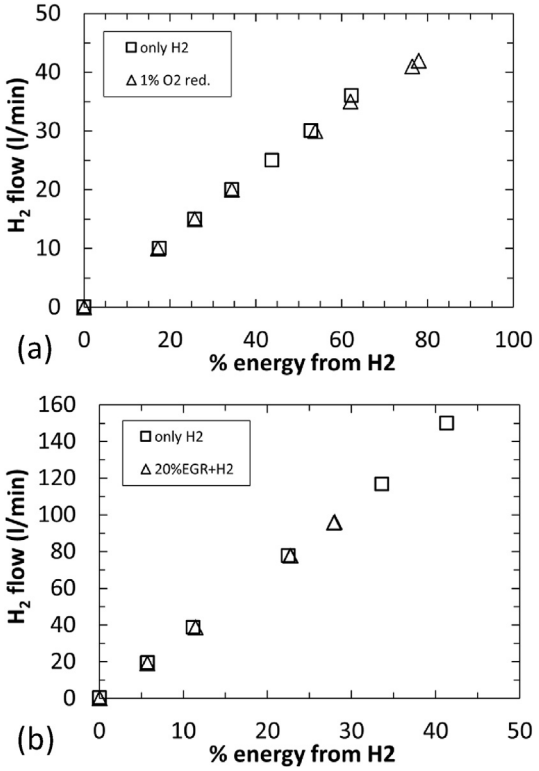

Fig. 3 – Percentage energy contribution from H_2 and the corresponding H_2 flow rates (l/min) for the (a) light duty diesel engine tests and (b) heavy duty diesel engine tests.

The charge air was regulated via a set of critical flow nozzles between the air supply reservoir and engine. The engine air mass flow is thus determined by the pressure upstream of the nozzles and is independent of the engine inlet pressure as long as the nozzles remain in the critical condition. This enabled the air mass flow to be held constant as more hydrogen was added to the inlet manifold. Exhaust emission were measured using a Horiba Mexa 7170 and particulate emissions with an AVL 415s smoke meter. Diesel fuel consumption was measured using an AVL 733 fuel balance.

Experimental methodology

The same specification of fuel was used across the two experimental facilities. The fossil diesel (RF-06-08 B5) used had 5.3% FAME (fatty acid methyl ester) content, a carbon to hydrogen mass ratio of 6.73:1 and cetane number of 52.7. The compressed H_2 used had a purity of 99.995%, while the compressed N_2 was of 99.5% purity. Table 3 lists lower heating values and densities of the fuels used in the tests.

Light duty diesel engine tests

For the light duty diesel engine tests, the engine speed was kept fixed at 1200 rpm, the diesel fuel was injected at a constant pressure of 600 bar and injection timing of 9 CAD BTDC. The injection timing was selected so that for the diesel only condition, the start of combustion (SOC) occurred at piston TDC.

Two sets of hydrogen-diesel fuel co-combustion were tests carried out on the light duty diesel engine. For both sets, the engine output load was fixed at 6.5 bar IMEP, which was achieved by varying the amount of diesel fuel and hydrogen supplied to the engine for each test to keep the IMEP constant. For the first set of tests, the engine was run in its naturally aspirated mode without any intake air boost or EGR. For the second set of tests, EGR-like conditions were simulated in the engine cylinder by aspirating N_2 gas in the intake flow to reduce the O_2 concentration in the intake air by 1%. The measured flow rates of N_2, H_2 and intake air were used to determine the reduction in O_2 concentration (v/v) due to the aspirated N_2. The temperature of the gas mixture in the intake manifold was 30 ± 1 °C for all the tests, measured 200 mm upstream of the inlet valve. Fig. 3(a) shows the percentage ratio of the energy supplied to the engine from H_2 to the total energy (i.e., energy from diesel fuel + H_2) and the corresponding H_2 flow rates.

Heavy duty diesel engine tests

For the heavy duty test programme, the A50 key point from the European Stationary Cycle (ESC) was selected. The A50 point on the drive cycle equates to a speed of 1250 rpm and 195 Nm of torque (50% load, 12 bar BMEP) on this engine. Four test conditions were selected; zero EGR and 20% EGR, and then both conditions with the start of combustion phased to TDC and then 10° after TDC. The start of fuel injection was varied to phase the start of combustion to TDC. In all cases, the engine was initially set up to a 25:1 AFR without hydrogen. The air mass flow into the engine was then held constant as hydrogen was added to the combustion chamber. The diesel fuel injection period was reduced to maintain constant load. As more hydrogen is added to the inlet manifold, the inlet manifold pressure would therefore rise but the oxygen available for combustion would remain constant. EGR was also set up with the engine operating only on diesel and measured via the Mexa 7000 by comparison of the CO_2 balance between the inlet and exhaust. The back pressure on the engine was maintained at 1.1 bar throughout the programme. The energy contribution from increased quantities of hydrogen for this set up are shown in Fig. 3(b).

Results and discussion

Combustion characteristics

Fig. 4 shows the in-cylinder gas pressure traces for both the light and heavy duty diesel engine tests. It can be clearly seen from the figure that the peak pressure increase when H_2 is added, as a result of H_2 co-combusting with the diesel fuel. Fig. 5(a) shows the apparent heat release rates from the H_2-diesel co-combustion tests carried out on the light duty diesel engine. The proportion of H_2 being added to the intake air was varied (between 0 and 20% H_2 v/v), but engine output load (IMEP) was kept constant at 6.5 bar IMEP by adjusting the amount of diesel fuel being injected into the engine cylinder. The results shown in Fig. 5(a) are with N_2 also being added to the intake manifold to reduce the intake O_2 concentration by

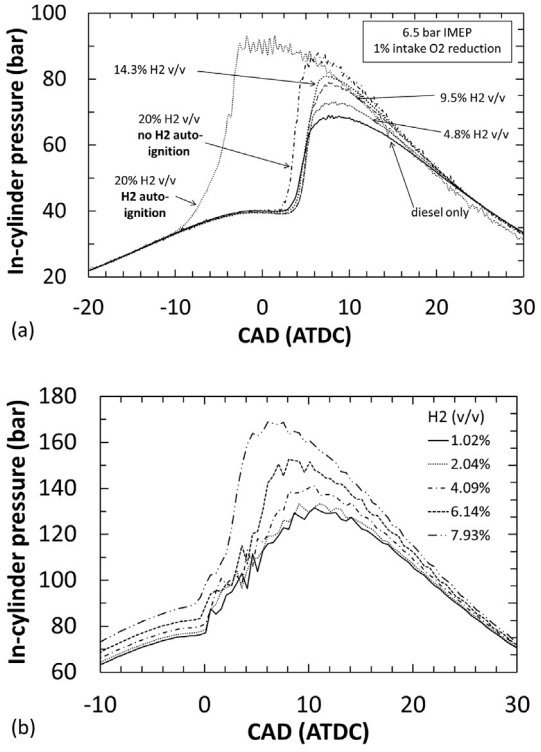

Fig. 4 – In-cylinder gas pressure traces for H_2-diesel co-combustion in (a) light duty diesel engine and (b) heavy duty diesel engine for different H_2 concentrations (by volume) in the intake air.

1% and simulate EGR-like conditions inside the cylinder. It can be seen from the figure that as the proportion of H_2 in the intake air is increased up to 20% v/v, the peak heat release rates increase resulting in a greater premixed burn fractions and, therefore, smaller diffusion-controlled burn fractions. The higher peak heat release rates and greater premixed burn fractions could be attributed to the H_2 being well mixed with the air, and upon diesel ignition the premixed H_2-air mixture (close to the diesel ignition sites) started combusting resulting in high rates of pressure rise and heat release close to the piston TDC position. In comparison, for the diesel only condition, a finite amount of diesel fuel is mixed with the air to combustible limits during the ignition delay period, which then burns resulting in the premixed burn stage. The rate of burning of the remainder of the intake charge depends on the diffusion-controlled mixing of remaining diesel fuel with air. At the highest tested H_2 concentration of 20% v/v in air, a reduction in the ignition delay period was observed, which resulted in the peak heat release occurring earlier than the diesel only condition. An interesting phenomenon was observed at the H_2 concentration of 20% v/v in air, whereby for some of the engine cycles the pressure rise (and heat release) was seen to occur even before diesel fuel injection had started, as can be seen in Figs. 4(a) and 5(a). Approximately 5% of the cycles underwent this phenomenon. It was thought that this was likely due to the H_2 auto-igniting, most probably due to the presence of a hot spot in the engine cylinder.

Fig. 5(b) shows the heat release rate curves for the H_2-diesel co-combustion experiments conducted on the heavy duty diesel engine. Above 8% hydrogen (v/v), an aggressive knocking type of combustion was observed, and data was therefore not gathered at these conditions to prevent damage to the engine. Previous studies have statistically investigated considered the relationship between cyclic variability and various fuel injection parameters [42], and future work could follow a similar approach so as to better understand and potentially control the occurrence of knock with H_2-diesel co-combustion. It can be seen from Fig. 5(b) that without H_2 addition, the bulk of heat release occurs during the mixing or diffusion controlled burn phase, with a smaller premixed burn phase immediately following the start of combustion. As the H_2 concentration is increased, the proportion of energy release during the initial premixed burn phase decreases and the magnitude of peak heat release rate during the second combustion phase (which is diffusion burn dominated at zero H_2 addition) increases, and at a H_2 addition level of 7.93%, the initial premixed burn phase originally apparent is no longer present. It can also be seen that as the level of H_2 addition increases, that peak heat release rates occur earlier during combustion (Fig. 5b), as was also observed in the case of the light duty engine tests (Fig. 5a). In the case of the heavy duty engine tests, it is suggested that the changes in combustion phasing with increased H_2 concentration (Fig. 5b) occur due to the increased availability of H_2 premixed with air at stoichiometries sufficient for rapid flame propagation following autoignition of the diesel fuel present. It is also possible that the increased rates of heat release rate with increased H_2 level may also, in part, be attributable to an increase in the charge density due to increasing boost pressure. It is therefore hypothesised that at the highest H_2 addition level of 7.93% in the heavy duty engine (Fig. 5b) that the first phase of

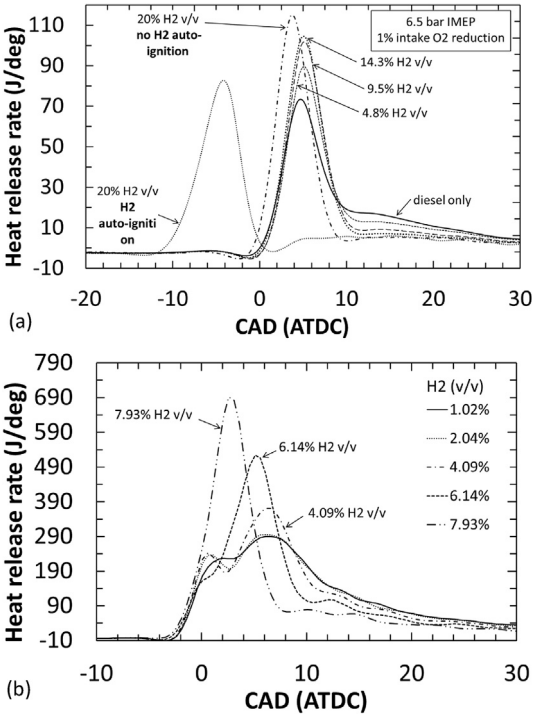

Fig. 5 – Apparent heat release rates for H_2-diesel co-combustion in (a) light duty diesel engine and (b) heavy duty diesel engine for different H_2 concentrations (by volume) in the intake air.

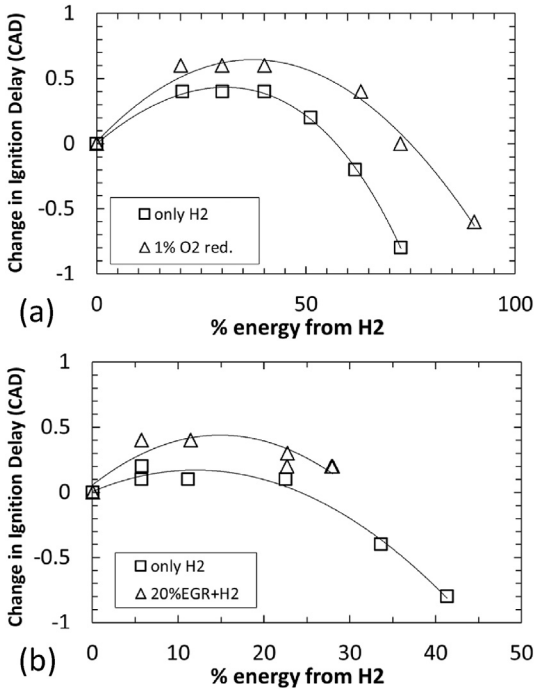

Fig. 6 – Change in ignition delay (w.r.t. diesel only condition) for H_2-diesel co-combustion tests on (a) light duty diesel engine and (b) heavy duty diesel engine for different percentage energy contribution from H_2.

combustion, during which the bulk of energy release occurs, is now dominated by heat release from premixed H_2, with heat release during diffusion controlled combustion of diesel fuel much reduced relative to the 0% H_2 addition case due to the displacement of diesel with H_2, and probable increased rates of diesel-air premixing due to heat release from H_2 in the initial combustion phase.

It is also possible that the increase in peak heat release rates in the heavy duty diesel engine could be attributable to the observation, that as H_2 is added, the bulk of combustion starts to move closer to the piston TDC position. This results in combustion occurring under increasingly lower cylinder volumes and therefore lower energy losses through surface heat transfer. A further possible explanation for the increased rates of heat release apparent is the autoignition of H_2 at multiple sites throughout the in-cylinder charge. However, it is interesting to note that if H_2 autoignition did occur in the heavy duty engine at 7.93% v/v H_2, then this is significantly lower than the level of 20% v/v at which H_2 autoignition occurred in the light duty engine. At these conditions, the bulk charge temperature is lower than the autoignition temperature and so other factors must contribute to autoignition. Local hot spots on the combustion chamber wall, or hot particle matter such as soot or oil are inevitable and could act as ignition sites. The heavy duty engine was of an iron piston and head construction where as the light duty engine had aluminium components. The heavy duty engine would therefore be expected to run at a higher combustion chamber surface temperature due to the iron construction and higher test load, which would explain the earlier transition to autoignition.

Fig. 6 shows the change in ignition delay (w.r.t. diesel only condition) as the amount of energy from the H_2 is increased (and the energy contribution from diesel fuel is decreased to maintain a constant engine load output). Ignition delay has been defined as the duration between the start of diesel fuel injection (SOI, the time at which the fuel injector actuation signal is sent) and the start of combustion (SOC), which is determined as the time at which the first detectable incidence of heat release occurs following diesel auto-ignition. For each of the light and heavy duty diesel engine tests, two operating conditions are shown in Fig. 6, the engine being operated without any EGR and then the engine being operated with EGR (in the case of the light duty diesel engine, EGR-like conditions were simulated inside the cylinder by using N_2 gas to reduce the intake O_2 concentration). It can be observed from Fig. 6 that there is a general trend, in the case of both light and heavy duty engine tests, whereby the increase in H_2 energy results in the ignition delay period initially increasing and subsequently decreasing with further H_2 addition. The initial increase in ignition delay could be attributed to the aspirated H_2 displacing the intake O_2, slowing down the low temperature fuel breakdown reactions and delaying diesel fuel autoignition. As the H_2 concentration in the intake air is increased, the in-cylinder H_2-air mixture becomes less lean.

The combustion of this increasingly less lean H_2-air mixture, close to engine TDC position results in higher rates of heat release (as can be seen in Fig. 5) and elevated in-cylinder temperatures, leading to a reduction in ignition delay. It could also be speculated that as the in-cylinder H_2-air mixture becomes less lean, the H_2 flame speed increases, which could

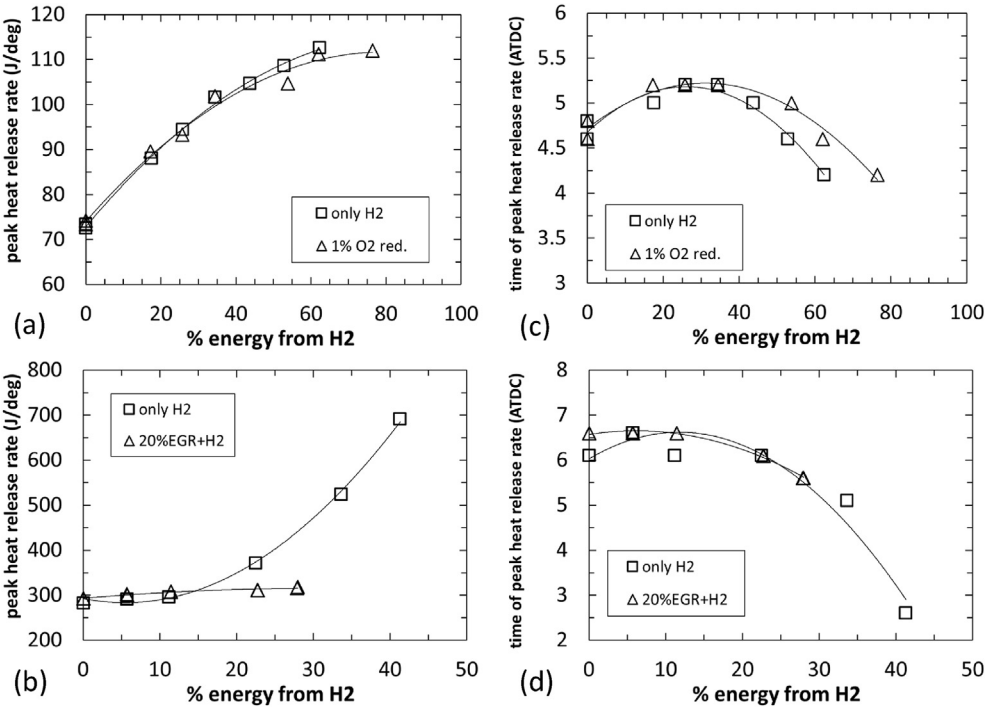

Fig. 7 – Peak heat release rates (J/deg) and time of peak heat release rates (ATDC) for H_2-diesel co-combustion tests carried out on a (a) and (c) light duty diesel engine and (b) and (d) heavy duty diesel engine, for different percentage energy contribution from H_2.

explain the higher rates of pressure rise and heat release at higher H_2 concentrations. The ignition delay results for the light duty engines tests (Fig. 6a) shows that the ignition delay period for the 1% intake O_2 reduction condition is generally higher as compared to the only H_2 test case. This could also be attributed to the additional N_2 further diluting the intake mixture and reducing the O_2 available for fuel combustion.

Fig. 7(a) and (b) show the peak heat release rates for the H_2-diesel co-combustion tests carried out on the light and heavy duty diesel engines, respectively. It can be seen that in general, the peak heat release rates increase as the H_2 energy contribution is increased. The reasons for this – premixed H_2-air mixture becoming less lean, leading to higher rates of pressure rise and heat release – have been explained in detail in the discussion for Fig. 5. In Fig. 7(a), peak heat release rates were slightly lower for the 1% intake O_2 reduced condition. An exception to this general trend can be observed in Fig. 7(b) for the tests carried out with 20% EGR where the change in H_2 concentration does not seem to have a significant effect on the peak heat release rate. This could be speculated to be due to the EGR reducing the intake O_2 concentration and lowering the in-cylinder gas temperatures. Therefore, the EGR could most likely offset the elevation of in-cylinder temperatures caused due to H_2 combustion, and thereby not net change in the peak heat release rates was observed. It is also worth mentioning the upswing in the rate of heat release curve observed for the no EGR case could still occur at higher hydrogen concentrations which were not studied due to the risk of undesired ignition occurring in the inlet system in the presence of EGR above 4% (v/v)

Fig. 7(c) and (d) show the time of peak heat release rates (tPHRR) for both the test setups. It can be seen from these graphs that the trend of the tPHRR plots follows the trend observed for the ignition delay in Fig. 6. This is expected as the change in the ignition delay period accordingly changes the combustion phasing and hence, the time of peak heat release. Furthermore, similar to the ignition delay trends observed in Fig. 6(a), the time of peak is earlier for the only H_2 case, the reasons for which have been explained in the discussion for Fig. 6.

Fig. 8a and b shows the calculated in-cylinder global temperatures with varying H_2 addition levels, with and without simulated EGR in the light duty engine. It can be seen from Fig. 8 that an increasing level of intake aspirated H_2 results in an increase in peak global temperatures, with and without the presence of simulated EGR, and that the maximum temperature is reached earlier following SOC. This is in agreement with the observed peak heat release rates (Fig. 7a), which increased with the increasing percentage of energy from H_2, with and without simulated EGR. Fig. 8b shows very little difference in temperatures reached with and without the use of simulated EGR, at a constant H_2 addition levels, which can likely be attributed to the use of N_2 aspiration for simulated EGR. Also apparent in Fig. 8 is a trend of increasing temperature from compression only, at approximately TDC and just prior to SOC. This can likely be attributed to the volumetric displacement of intake air with H_2, and the subsequent change in the intake mixture ideal gas constant.

Fig. 9 shows the calculated in-cylinder global temperatures with varying H_2 addition levels, with and without EGR in the

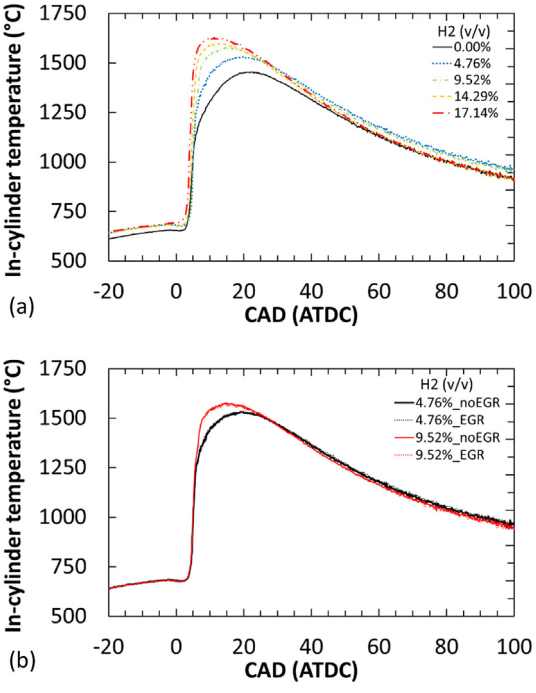

Fig. 8 – In-cylinder global temperature for light duty (a) no EGR, (b) comparison between EGR and no EGR tests for two H_2 proportions.

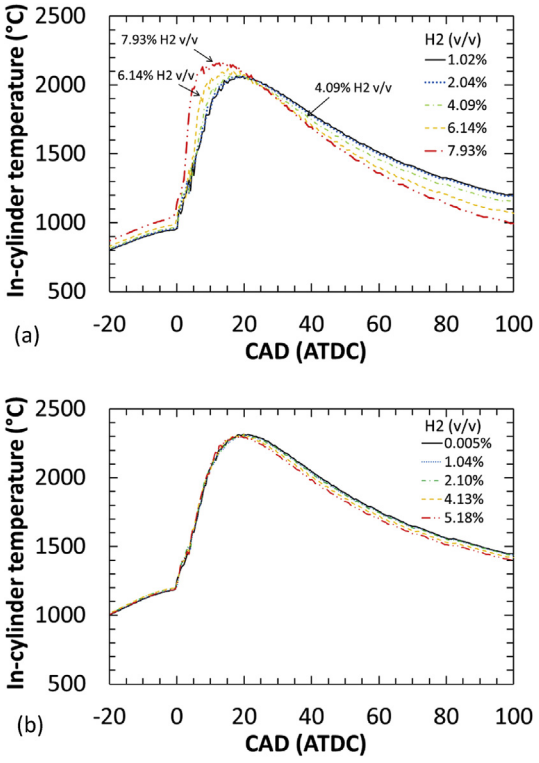

Fig. 9 – In-cylinder global temperature for heavy duty (a) no EGR, (b) EGR.

heavy duty engine. It can be seen that when the engine was operated without EGR (Fig. 9a) that peak in-cylinder global temperatures increased with an increasing level of H_2 addition, as was also observed in the light duty engine tests (Fig. 8a). However, with the use of EGR (Fig. 9b), the effect of H_2 addition on peak temperatures is significantly less pronounced. It is suggested that this can be attributed to the decreased availability of O_2, decreasing rates of additional heat release and temperature increase from H_2, as indicated by the observed peak heat release rates (Fig. 7b). Fig. 9a also shows that as the increase in aspirated H_2 levels resulted in higher in-cylinder temperatures, in-cylinder temperatures subsequently reduced more rapidly than at lower H_2 levels, in agreement with the observed changes in combustion phasing, where the bulk of energy release occurred earlier with increasing H_2 levels. A similar, but much less pronounced, trend can be seen in the light-duty in-cylinder temperatures, where temperatures in the case of the highest H_2 addition level (17.14% v/v) decreased more rapidly to the same level as the diesel only case (Fig. 8a).

Fig. 10 shows the indicated thermal efficiencies with varying proportions of energy from H_2, with and without EGR, of the light duty and heavy duty engines. It can be seen in Fig. 10a that there is a decrease in indicated thermal efficiency with an increasing proportion of energy from H_2 in the heavy duty engine. This is in agreement with previous studies [35,36] and can likely be attributed to the comparatively high levels of the aspirated H_2 persisting unburnt to the exhaust gases relative to that of the diesel fuel. However, in the case of the light duty engine (Fig. 10b), such a decrease can only be observed where no simulated EGR (1% O_2 reduction) was included, and an increase in indicated thermal efficiency at levels of energy from H_2 of between 60% and 90% can instead be observed. It is tentatively suggested that this may be attributable to greater detrimental effect of O_2 reduction on diesel combustion efficiency relative to that of H_2, and a concurrent increase in H_2 combustion efficiency due to an increase in the H_2 air equivalence ratio with an increasing proportion of energy from H_2.

Exhaust emissions

Fig. 11 shows the specific exhaust emissions of CO from H_2-diesel fuel co-combustion tests carried out on both light and heavy duty diesel engines. The observed trends in CO exhaust emissions are very similar with both test setups (notwithstanding the range of reproducibility present in Fig. 11b at 0% energy from diesel), in that an almost linear reduction in the gaseous emissions is observed as the percentage energy contribution from H_2 is increased. This reduction in carbon emissions is expected as diesel fuel is replaced by H_2 which does not produce CO as a combustion product.

When comparing the CO emissions between the light and heavy duty diesel engines (Fig. 11), it is interesting to note that CO emissions are lower for the heavy duty diesel engine, as compared to the light duty. This could potentially be due to the higher in-cylinder gas temperatures in the heavy duty

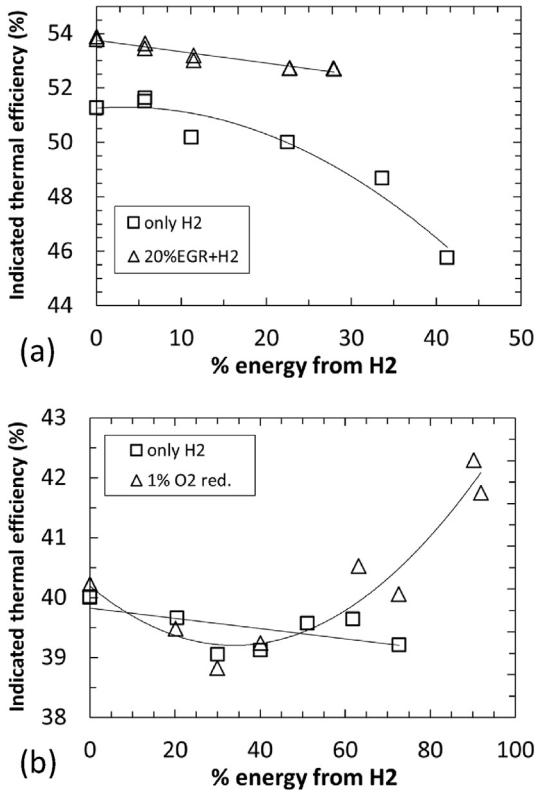

Fig. 10 – Indicated thermal efficiency in (a) heavy duty, and (b) light duty, with varying proportion of energy from H_2.

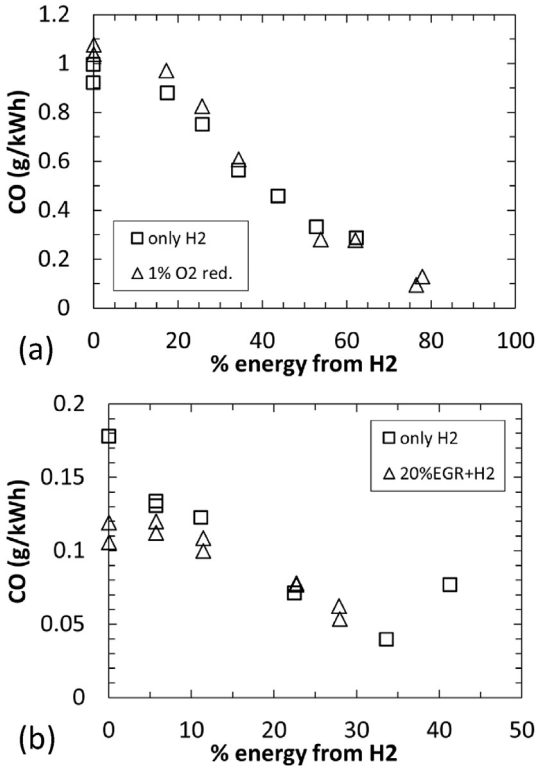

Fig. 11 – Specific exhaust emissions of CO (g/kWh) for H_2-diesel co-combustion tests carried out on a (a) light duty diesel engine and (b) heavy duty diesel engine, for different percentage energy contribution from H_2.

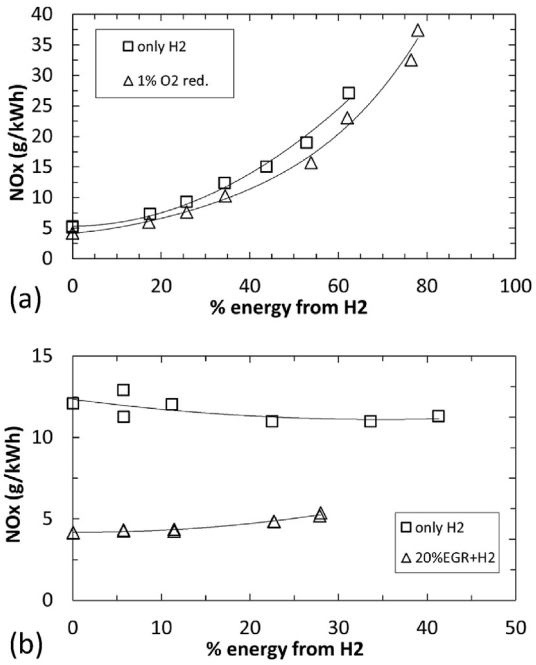

Fig. 12 – Specific exhaust emissions of NO_x (g/kWh) for H_2-diesel co-combustion tests carried out on a (a) light duty diesel engine and (b) heavy duty diesel engine, for different percentage energy contribution from H_2.

diesel engine resulting in higher rates of diesel fuel oxidation to CO_2, and therefore lower CO emissions.

Fig. 12(a) and (b) show the specific NO_x emissions from H_2-diesel co-combustion tests carried out on the light and heavy duty diesel engines respectively. First considering the NO_x emissions from the light duty diesel engine (Fig. 9a), it can be seen that as the diesel fuel is substituted by H_2, a consistent increase in NO_x emissions is observed. This increase in NO_x emissions agrees with the peak heat release and in-cylinder global temperature trends observed in Figs. 7a and 8a respectively, where an increase in both peak heat release rates and maximum in-cylinder global temperatures was observed with increasing H_2 concentration (or increasing percentage H_2 energy contribution). This is to be expected as NO_x formation rates in CI combustion are governed by the reactions of the extended Zeldovich mechanism, with conditions of high temperatures and high O_2 concentrations resulting in high NO formation rates [43,44]. When considering the NO_x emissions from the heavy duty diesel engine (Fig. 12b), the diesel only levels without EGR are higher than for the light duty case (Fig. 12a), supporting the case that the combustion chamber runs hotter due to the higher load and higher chamber wall temperatures. It might have been expected that the NO_x emissions of the heavy duty with increasing energy from H_2 would increase in the same manner (as for the light duty) since the peak heat release rates (Fig. 7b, heavy duty engine tests, only H_2 case) and in-cylinder global temperatures (Fig. 9a) both increased with increasing H_2 concentration. However, in contrast, NO_x emissions (Fig. 12b) showed a slight reduction with increasing percentage energy from H_2. The net NOx emissions are formed from a large contribution from the diesel diffusion flame and lower contribution from the lean, homogenous combustion of the hydrogen – air mixture. In the heavy duty case, the air-fuel ratio was held constant so which has the effect of making the hydrogen mixture very lean and provides more heat capacity to absorbed the heat released from combustion. The NOx contribution from homogenous combustion will therefore be low due to high dilution levels and the excess air may reduce the overall temperature rise in the diffusion flame. Notwithstanding the assumptions made in calculating in-cylinder global temperatures, it is suggested that the observed increased rate of temperature decrease following a maximum (Figs. 8a and 9a) provides some support for lower temperatures in the diffusion flame as H_2 levels increase. How these complex factors interact is the subject of ongoing research.

Fig. 13a shows the specific exhaust emissions of the unburned total hydrocarbons (THC) in the light duty diesel engine. It can be observed from the figure that THC emissions increase with increasing energy of H_2, most likely due to the reduction in intake O_2. Fig. 13b shows the specific exhaust emissions of the total particulate mass (TPM) from the H_2-diesel fuel co-combustion tests conducted on the light duty diesel engines. It can be seen from Fig. 13b that as the percentage energy contribution from H_2 is increased (and that from diesel fuel is decreased to maintain a constant engine load), a considerable reduction in TPM emissions is observed to 25% of their original value when the percentage energy contribution from H_2 was increased to 20%. In the case of the

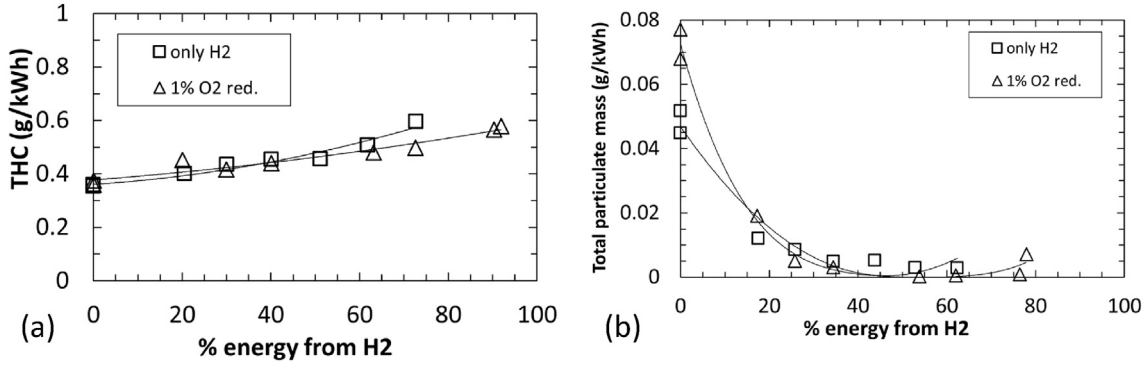

Fig. 13 – Specific exhaust emissions of (a) unburned total hydrocarbons (THC) and (b) total particulate mass (g/kWh) for H_2-diesel co-combustion tests carried out on a light duty diesel engine for different percentage energy contribution from H_2.

heavy duty diesel engine, at all operating conditions PM emissions were below the instrument detection limit. As discussed in the context of CO emissions (Fig. 11), the reduction in particulate emissions is expected as diesel fuel is replaced by H_2.

Conclusions

1. For both light and heavy duty diesel engine tests, the ignition delay was observed to initially increase as H_2 was added and subsequently decrease with further H_2 addition. The initial increase in ignition delay was attributed to the dilution of the intake air by H_2 and N_2, while the subsequent reduction was due to elevated in-cylinder gas temperatures from H_2 combustion.
2. Peak heat release rates also increased with increasing H_2 concentration. This was attributed to the increase in the in-cylinder H_2-air stoichiometry leading to high rates of heat release closer to engine TDC position with increasing levels of H_2 combustion.
3. In the case of the light duty engine tests, H_2 was observed to auto-ignite intermittently before diesel fuel injection had started, when the H_2 concentration in air was 20% v/v. It is thought that this phenomenon likely occurred due to the presence of a hot spot inside the cylinder. In the heavy duty engine, significantly increased and advanced rates of heat release were observed at a lower H_2 concentration of 8% v/v, possibly aided by the higher operating temperatures of the heavy duty engine relative to those of the light duty engine.
4. NO_x emissions were seen to follow the trend of the peak heat release rates and increase with increasing H_2 concentration in the case of the light duty engine tests. However, in contrast, for the heavy duty tests, NO_x emissions stayed constant/reduced slightly with increasing H_2 levels, potentially attributable to lower temperatures during diffusion controlled combustion, despite an increase in peak heat release rates during premixed combustion.
5. CO and particulate mass emissions were observed to decrease as the energy contribution from H_2 was increased, and that from diesel fuel (and thus fuel carbon supplied) was decreased to maintain a constant engine load.

It can be seen that while similar effects of H_2 intake aspiration, and displacement of energy from diesel fuel, on the duration of ignition delay and combustion phasing were observed in both a light duty and heavy duty engine, the impact of these effects differed. For example, in the light duty engine operating at medium load, NOx emissions correlated closely with peak heat release rates during the premixed burn fraction, whereas in the heavy duty engine at a higher load, NOx emissions showed a greater influence of temperatures during diffusion controlled combustion. Therefore, while H_2 has potential for reducing carbon based emissions from both light and heavy duty diesel engines, the degree to which H_2 co-combustion can be implemented without undesired H_2 auto-ignition or elevated NOx is dependent on engine design and operating conditions.

Acknowledgements

The authors would also like to acknowledge EPRSC (EP/M009424/1 and EP/M007960/1) and Innovate UK (Heatwave II-101560) for their support to this project.

Nomenclature

ATDC	after-top-dead-centre
BDC	bottom dead centre
BMEP	brake mean effective pressure
BTDC	before-top-dead-centre
BTE	brake thermal efficiency
CAD	crank angle degree
CI	compression ignition
CO	carbon monoxide
CO_2	carbon dioxide
EGR	exhaust gas recirculation
H_2	hydrogen
IMEP	indicated mean effective pressures
NO_x	nitrogen oxides
O_2	oxygen
PM	particulate mass
ppr	pulses per revolution
rpm	revolutions per minute
SOC	start of combustion
SOI	start of injection
TDC	top-dead-centre
THC	total hydrocarbons

REFERENCES

[1] Viewpoint: The trouble with diesel - BBC News n.d. http://www.bbc.co.uk/news/science-environment-38814297 [Accessed 2 February 2017].
[2] C40 Cities. C40 Blog - daring cities make bold air quality commitment to remove all diesel vehicles by 2025. 2016. http://www.c40.org/blog_posts/daring-cities-make-bold-air-quality-commitment-to-remove-all-diesel-vehicles-by-2025. [Accessed 2 February 2017].
[3] Gosling SN, Arnell NW. A global assessment of the impact of climate change on water scarcity. Clim Change 2016;134:371–85. https://doi.org/10.1007/s10584-013-0853-x.
[4] Zecca A, Chiari L. Fossil-fuel constraints on global warming. Energy Pol 2010;38:1–3. https://doi.org/10.1016/j.enpol.2009.06.068.
[5] McGlade C, Ekins P. The geographical distribution of fossil fuels unused when limiting global warming to 2°C. Nature 2015;517:187–90. https://doi.org/10.1038/nature14016.
[6] Sarlioglu B, Morris CT, Han D, Li S. Driving toward accessibility: a review of technological improvements for electric machines, power electronics, and batteries for electric and hybrid vehicles. IEEE Ind Appl Mag 2017;23:14–25. https://doi.org/10.1109/MIAS.2016.2600739.
[7] Hofmann J, Guan D, Chalvatzis K, Huo H. Assessment of electrical vehicles as a successful driver for reducing CO2 emissions in China. Appl Energy 2016;184:995–1003. https://doi.org/10.1016/j.apenergy.2016.06.042.
[8] Ellingsen LA-W, Singh B, Strømman AH, C B, GROUP B, al BT et al ed EO et, et al. The size and range effect: lifecycle greenhouse gas emissions of electric vehicles. Environ Res

Lett 2016;11:54010. https://doi.org/10.1088/1748-9326/11/5/054010.
[9] Sen B, Ercan T, Tatari O. Does a battery-electric truck make a difference? – Life cycle emissions, costs, and externality analysis of alternative fuel-powered Class 8 heavy-duty trucks in the United States. J Clean Prod 2017;141:110–21. https://doi.org/10.1016/j.jclepro.2016.09.046.
[10] Dec JE. A conceptual model of DI diesel combustion based on laser-sheet imaging. SAE Pap 1997:970873. https://doi.org/10.4271/970873.
[11] Tree DR, Svensson KI. Soot processes in compression ignition engines. Prog Energy Combust Sci 2007;33:272–309. https://doi.org/10.1016/j.pecs.2006.03.002.
[12] Eveleigh A, Ladommatos N, Hellier P, Jourdan A-L. An investigation into the conversion of specific carbon atoms in oleic acid and methyl oleate to particulate matter in a diesel engine and tube reactor. Fuel 2015;153:604–11. https://doi.org/10.1016/j.fuel.2015.03.037.
[13] Ladommatos N, Rubenstein P, Bennett P. Some effects of molecular structure of single hydrocarbons on sooting tendency. Fuel 1996;75:114–24.
[14] Hellier P, Ladommatos N. The influence of biodiesel composition on compression ignition combustion and emissions. Proc Inst Mech Eng Part A J Power Energy 2015;229:714–26. https://doi.org/10.1177/0957650915598424.
[15] Rakopoulos DC, Rakopoulos CD, Giakoumis EG. Impact of properties of vegetable oil, bio-diesel, ethanol and n-butanol on the combustion and emissions of turbocharged HDDI diesel engine operating under steady and transient conditions. Fuel 2015;156:1–19. https://doi.org/10.1016/j.fuel.2015.04.021.
[16] Peirce DM, Alozie NSI, Hatherill DW, Ganippa LC. Premixed burn fraction: its relation to the variation in NO x emissions between petro- and biodiesel. Energy Fuels 2013;27:3838–52. https://doi.org/10.1021/ef4006719.
[17] Rakopoulos DC, Rakopoulos CD, Kyritsis DC. Butanol or DEE blends with either straight vegetable oil or biodiesel excluding fossil fuel: comparative effects on diesel engine combustion attributes, cyclic variability and regulated emissions trade-off. Energy 2016;115:314–25. https://doi.org/10.1016/J.ENERGY.2016.09.022.
[18] Herreros JM, Schroer K, Sukjit E, Tsolakis A. Extending the environmental benefits of ethanol–diesel blends through DGE incorporation. Appl Energy 2015;146:335–43. https://doi.org/10.1016/j.apenergy.2015.02.075.
[19] Wei L, Geng P. A review on natural gas/diesel dual fuel combustion, emissions and performance. Fuel Process Technol 2016;142:264–78. https://doi.org/10.1016/j.fuproc.2015.09.018.
[20] Mobasheri R, Seddiq M, Peng Z. Separate and combined effects of hydrogen and nitrogen additions on diesel engine combustion. Int J Hydrogen Energy 2018;43:1875–93. https://doi.org/10.1016/J.IJHYDENE.2017.11.070.
[21] Tsujimura T, Suzuki Y. The utilization of hydrogen in hydrogen/diesel dual fuel engine. Int J Hydrogen Energy 2017;42:14019–29. https://doi.org/10.1016/J.IJHYDENE.2017.01.152.
[22] Aldhaidhawi M, Chiriac R, Bădescu V, Descombes G, Podevin P. Investigation on the mixture formation, combustion characteristics and performance of a diesel engine fueled with diesel, biodiesel B20 and hydrogen addition. Int J Hydrogen Energy 2017;42:16793–807. https://doi.org/10.1016/J.IJHYDENE.2017.01.222.
[23] Saravanan N, Nagarajan G, Sanjay G, Dhanasekaran C, Kalaiselvan KM. Combustion analysis on a DI diesel engine with hydrogen in dual fuel mode. Fuel 2008;87:3591–9. https://doi.org/10.1016/j.fuel.2008.07.011.
[24] Christodoulou F, Megaritis A. Experimental investigation of the effects of separate hydrogen and nitrogen addition on the emissions and combustion of a diesel engine. Int J Hydrogen Energy 2013;38:10126–40. https://doi.org/10.1016/j.ijhydene.2013.05.173.
[25] Tomita E, Kawahara N, Piao Z, Fujita S, Hamamoto Y. Hydrogen combustion and exhaust emissions ignited with diesel oil in a dual fuel engine. SAE Pap 2001. https://doi.org/10.4271/2001-01-3503. 2001–01–3503.
[26] Tsolakis A, Hernandez JJ, Megaritis A, Crampton M. Dual fuel diesel engine operation using H 2. Effect on particulate emissions. Energy Fuels 2005;19:418–25. https://doi.org/10.1021/ef0400520.
[27] Talibi M. Co-combustion of diesel and gaseous fuels with exhaust emissions analysis and in-cylinder gas sampling. PhD Thesis (Doctoral),University College London; 2015.
[28] Varde KS, Varde LK. Reduction of soot in diesel combustion with hydrogen and different H/C gaseous fuels. Toronto, Canada: 5th World Hydrog. Energy; 1984.
[29] Miyamoto T, Hasegawa H, Mikami M, Kojima N, Kabashima H, Urata Y. Effect of hydrogen addition to intake gas on combustion and exhaust emission characteristics of a diesel engine. Int J Hydrogen Energy 2011;36:13138–49. https://doi.org/10.1016/j.ijhydene.2011.06.144.
[30] Talibi M, Hellier P, Ladommatos N. The effect of varying EGR and intake air boost on hydrogen-diesel co-combustion in CI engines. Int J Hydrogen Energy 2016. https://doi.org/10.1016/j.ijhydene.2016.11.207.
[31] Roy MM, Tomita E, Kawahara N, Harada Y, Sakane A. An experimental investigation on engine performance and emissions of a supercharged H2-diesel dual-fuel engine. Int J Hydrogen Energy 2010;35:844–53. https://doi.org/10.1016/j.ijhydene.2009.11.009.
[32] Banerjee R, Roy S, Bose PK. Hydrogen-EGR synergy as a promising pathway to meet the PM–NOx–BSFC trade-off contingencies of the diesel engine: a comprehensive review. Int J Hydrogen Energy 2015;40:12824–47. https://doi.org/10.1016/j.ijhydene.2015.07.098.
[33] Wu H-W, Hsu T-T, He J-Y, Fan C-M. Optimal performance and emissions of diesel/hydrogen-rich gas engine varying intake air temperature and EGR ratio. Appl Therm Eng 2017;124:381–92. https://doi.org/10.1016/j.applthermaleng.2017.06.026.
[34] Pana C, Negurescu N, Cernat A, Nutu C, Mirica I, Fuiorescu D. Experimental aspects of the hydrogen use at diesel engine. Procedia Eng 2017;181:649–57. https://doi.org/10.1016/j.proeng.2017.02.446.
[35] Liu S, Li H, Liew C, Gatts T, Wayne S, Shade B, et al. An experimental investigation of NO2 emission characteristics of a heavy-duty H2-diesel dual fuel engine. Int J Hydrogen Energy 2011;36:12015–24. https://doi.org/10.1016/j.ijhydene.2011.06.058.
[36] Liew C, Li H, Nuszkowski J, Liu S, Gatts T, Atkinson R, et al. An experimental investigation of the combustion process of a heavy-duty diesel engine enriched with H2. Int J Hydrogen Energy 2010;35:11357–65. https://doi.org/10.1016/j.ijhydene.2010.06.023.
[37] Morgan R, Atkins P, Atkins A, Lenartowicz C, Heikal M. Effect of hydrogen fumigation in a dual fueled heavy duty engine. SAE Tech Pap 2015. https://doi.org/10.4271/2015-24-2457.
[38] Shudo T, Yamada H. Hydrogen as an ignition-controlling agent for HCCI combustion engine by suppressing the low-temperature oxidation. Int J Hydrogen Energy 2007;32:3066–72. https://doi.org/10.1016/j.ijhydene.2006.12.002.
[39] Mohamed Ibrahim M, Ramesh A. Investigations on the effects of intake temperature and charge dilution in a hydrogen fueled HCCI engine. Int J Hydrogen Energy 2014. https://doi.org/10.1016/j.ijhydene.2014.07.019.
[40] Maurya RK, Akhil N. Comparative study of the simulation ability of various recent hydrogen combustion mechanisms

in HCCI engines using stochastic reactor model. Int J Hydrogen Energy 2017. https://doi.org/10.1016/j.ijhydene.2017.02.155.

[41] Mustafa IH, Fgaier H, Elkamel A, Lohi A, Ibrahim G, Elnashaie SSEH. Correction to effect of the feed substrate concentration on the dynamic performance of the bioethanol fermentation process using zymomonas mobiliz. Energy Fuels 2014;28:7746. https://doi.org/10.1021/ef502722u. 7746.

[42] Rakopoulos CD, Rakopoulos DC, Giakoumis EG, Kyritsis DC. The combustion of *n* -butanol/diesel fuel blends and its cyclic variability in a direct injection diesel engine. Proc Inst Mech Eng Part A J Power Energy 2011;225:289–308. https://doi.org/10.1177/2041296710394256.

[43] Miller JA, Bowman CTC. Mechanism and modeling of nitrogen chemistry in combustion. Prog Energy Combust Sci 1989;15:287–338. https://doi.org/10.1016/0360-1285(89)90017-8.

[44] Bowman CT. Kinetics of nitric oxide formation incombustion processes. Symp Combust 1973;14:729–38. https://doi.org/10.1016/S0082-0784(73)80068-2.